Measurement of Flash Intensity at the Muzzle of a Firearm and Possible Protection against its Effects

I. Pemcak[*1], K. Novackova[1], T. Balaz[1], J. Krejci[1] and I. Bulinova[2]

[1]*University of Defence, Brno, Czech Republic*
[2]*Czech Armed Forces*

Abstract:

The constant increase in sensitivity of night vision devices used as weapon sights means that the photocathode may be permanently degraded or overexposed, and microchannels may be "burned out" by muzzle flash of weapon firing. This is manifested by uneven sensitivity of the photocathode surface or black dots in the field of view. The aim of this paper is to analyze the magnitude of the risk of damage to the image intensifier tube by muzzle flash during a shot and, based on this analysis, to propose possible ways of protection of the image intensifier tube from the effects of muzzle flash during a shot.

1 Introduction

1.1 NVD Characteristics

The structural core of any Night Vision Device (NVD) is the Image Intensifier Tube (IIT), which amplifies the brightness of the image and partially transforms the near-infrared image into the visible spectrum. This technology is widely used in both civilian and military applications. In modern armies and in police forces, the use of NVDs is standard, both in the form of observation devices and in the form of rifle sights. NVD technology allows transformation and amplification of an input image invisible to the human eye into a visible output. The quality of individual IITs has improved over time with the development of new technologies and continuous improvements in manufacturing techniques and technologies. The effectiveness of each device is linked to the level of parameters and characteristics of the IIT. Since the end of World War II, the vast majority of NVDs have used IITs instead of previously used electro-optical converters (EOCs). The EOC function

---

* *Corresponding author: Department of Weapons and Ammunition, University of Defence, Kounicova 65, CZ-612 10, Brno, Czechia. Phone: +420 973 44 32 16. E-mail: ivan.pemcak@unob.cz, ORCID 0009-0000-2224-4792*

is described in the literature, so we will not deal with it in this work [1-3]. The functions of IIT are summarized in following paragraphs.

1.2 Image Intensifier Tubes

The light radiation (natural or artificial) reflected from the observed object passes through the NVD lens and hits the IIT photocathode. The process is schematically shown in Fig. 1. Here, the external photoelectric phenomenon of electron emission occurs. The electrons are carried by the voltage field into the microchannel plate (MCP). Here, electrons are reflected from the walls of the individual MCP channels, where the secondary emission of electrons (multiplication of their number) occurs. At the output of the MCP, the multiplied electrons land on the luminescent screen and excite the luminescence. The process is depicted in Fig. 1. This is a similar mechanism to that of CRT monitors. The photons emitted from a luminescent screen are very often guided by an optical fiber, which acts as a reversal system. The photons are emitted from the fiber optic by the eyepiece of the instrument. The photons density on the IIT photocathode are therefore amplified by multiplying the number of electrons. The whole process, which is much more complex, is described in the literature, and its details are beyond the scope of this paper [1, 2].

Traditionally, the quality of NVDs has been assessed and reported according to their so-called generations. Generations I and II used EOC and generations III and IV used IIT. Today, this division is outdated and other factors are used for evaluation. Due to the limited number of IIT manufacturers worldwide, the IIT type designation is usually used as a quality indicator. In the EU, the type IIT labelled XD-4 from Photonis is usually used for small, portable NVDs [4].

IITs of individual manufacturers are usually interchangeable in their category. That is, their external dimensions, power characteristics and the size of the photocathode and screen are compatible. They can therefore be replaced between NVDs as part of repairs, maintenance or upgrade.
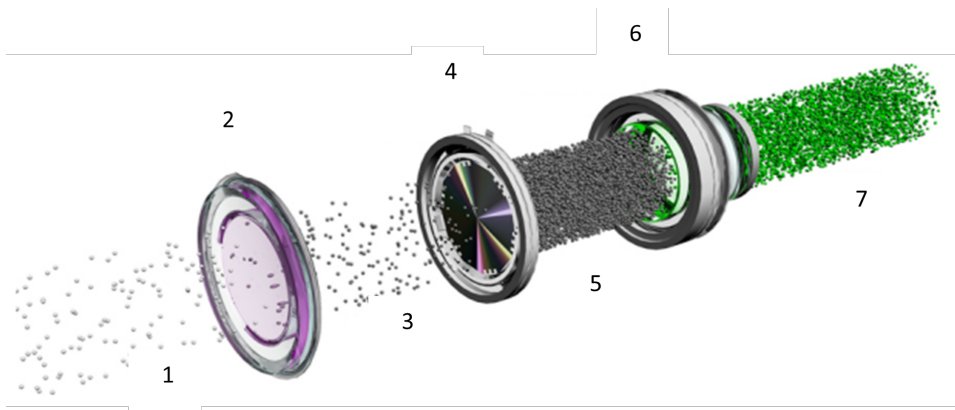

Fig. 1 Schematic of image intensifier tube [5]

1.3 Night Vision Opto-electronic System

The opto-electronic night system of NVD is based on the Kepler telescope system, which is equipped with an IIT in place of an optical inverting system. The location of the IIT in the optical system is designed so that the photocathode is located in the image focal plane of the objective and the luminescent shield in the object focal plane of the eyepiece.

Night sights are intended for aiming at a target in low light conditions, in the dark or at night. For the first time, night sights for handheld weapons were used at the end of the Second World War by German troops. Their weapon system consisted of an active infrared sight ZG 1229 (code name Vampir) and an assault rifle StG44 [6]. It was a bulky, complicated device. Thanks to technological progress, today's devices are much lighter and more compact. Night sights for small arms are currently designed either as stand-alone sights, as device installed in front of the main sight or as an addition for colimator sights.

## 2   Illumination of Objective Lens of NVD during Weapons Fire

Increasing the sensitivity of the IIT to enhance the range of the NVD has one major drawback. As the sensitivity of the IIT increases, there is a major increase in susceptibility to malfunction and damage. Secondary manifestations of a shot from a firearm are in particular a flash of light (primary and secondary) at the muzzle, caused by escaping powder gases and a peak acceleration caused by recoil (up to $5 \times 10^3 \, \mathrm{m \cdot s^{-2}}$). Many other phenomena related to the discharge of hot gases and unburned powder particles occur at the muzzle of the weapon, which present their own challenges in the field of weapon design. Malfunctions of NVD caused by the mechanical impulse of recoil are not exceptional, but less common. In this work, we will deal with the effects of the light radiation of burning powder gases coming out of the barrel [7, 8].

Most problematic is the use of NVD on weapons with short-barrels such as carbines and short-barreled rifles (SBRs). These guns often use a cartridge designed for longer barrels. As a result, the unburned powder grains burn up at the muzzle and a dominant flash occurs. As will be discussed later, the function of muzzle devices (flame suppressor, compensator) is usually beneficial for IIT protection but cannot be relied upon [9, 10].

Specific procedures have already been implemented to protect the photocathode and the entire device. One of the basic ways of protecting the IIT from damage is the autogating and automatic brightness control (ABC) function. Based on the feedback loop, it evaluates the intensity of captured light and after exceeding certain limit, it reduces the voltage on the MCP and therefore its brightness amplification. This feature is implemented "out of the box" in all modern IITs.

2.1 Experimental Measurment of Muzzle Flash Intensity

Experimental measuring of muzzle flash intensity was conducted in past. The aim of this paper is to use more available components than in other experiments [11]. To determine the light intensity on the input surface of the optoelectronic device, an experimental measurement was carried out using phototransistors as primary detectors. The location of the phototransistor is indicated in Fig. 2. First phototransistor (PT1) is positioned 9 cm above the bore and 25 cm from the muzzle. Therefore it is positioned right in front of first NVDs lens. The main axis of phototransistor is oriented in parallel with bore axis. The detection cone of the phototransistor was directed to the area of burning powder particles after
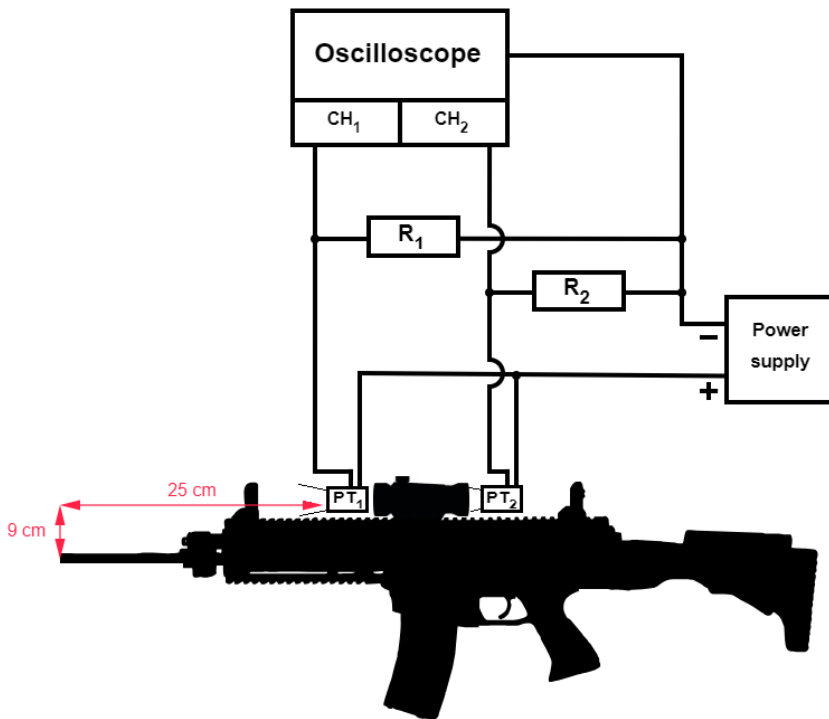
Fig. 2 Measuring diagram

weapon fire. As another part of the experiment, the delay of the autogating function during the shot was determined. Therefore, the second measuring phototransistor (PT2) was placed in the exit pupil of the NVD.

Fig. 3 shows the connection diagram of one of two measuring circuits, for measuring the intensity of the flash at the muzzle or behind NVD. Wiring diagram for both channels are identical. Due to the fact that usually an oscilloscope is not able to measure the current directly, an indirect measurement using a series-connected resistor or current probe have to be used.

Measuring chain was created twice, as detailed in Fig. 2. Parts used in measuring chain are listed below.

- 2 pcs – phototransistors LL 503PTC2E-1AD,
- 2 pcs – resistor 330 Ω,
- 1 pcs – 2-channel digital oscilloscope RTC 1002,
- 1 pcs – 2- channel programmable power supply M10-QD 3010.

A standard phototransistor without a base terminal type LL 503PTC2E-1AD from the manufacturer Luckylight was selected for the measurement. This phototransistor is sensitive in the spectral range $200 \div 1200$ nm. It is an NPN type silicon phototransistor
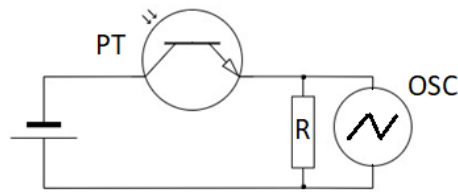
Fig. 3 Basic measuring schema

with an integrated clear lens with a diameter of 5 mm. This phototransistor has a sufficiently short time constant $T = 15\,\mu\text{s}$. The mentioned information is provided by the manufacturer [12].

The voltage was measured on the resistor connected in series with the phototransistor with an oscilloscope. From the knowledge of Ohm's law, the current flowing through the resistor was calculated. In earlier experiments, current probes were used, which are replaced with this resistor. This allowed an easier calibration of the measuring chain [2].

2.2 Calibration of Measuring Chain

To acuqire valid results measuring chain had to be calibrated before the measuring. A schematic of the calibration workstation is shown in Fig. 4. Main components are: a Luxmeter Vega from Ophir with measuring probe, a light source (halogen lamp) and a light integrating sphere with $d = 15\,\text{cm}$. The used light source produces light by heating a tungsten wire, which is theoretically close to an ideal blackbody in its properties. The radiation produced by the secondary flash at the muzzle of the gun is emitted by hot carbon particles, which are also theoretically close to an ideal blackbody. For the purposes of this work, the spectral properties of the two flashes were assumed to be identical. This simplification is only acceptable at this initial stage of protection design. For accurate results, it is necessary to calibrate the measurement chain directly to the spectrum emitted by the flash of a particular weapon, under specific conditions, using specific ammunition, which is difficult to do in practice [13].

The level of illumination was controlled by the aperture at the entrance to the integrating sphere. The size of the aperture was changed in steps, and each time the voltage value on the oscilloscope and the illumination value on the luxmeter were recorded, and at the same time, the phototransistor and the luxmeter probe were placed simultaneously in the measuring window of the integrating sphere. From these values, a calibration curve of the dependence of the illumination on the measured voltage was created. The shape of the calibration curve is close to an exponential function. Due to the range of measured values a logarithmic scale was used for Fig. 5.

Luxmeter was used to measure the intensity of illumination while the phototransistor worked in the visible and infrared light spectrum, thus recording the intensity of irradiation. The use of photometric quantities for evaluating IIT properties is not uncommon. The sensitivity of a photocathode is usually measured using the photometric quantity A/lm. This discrepancy was due to an imperfection in the measurement method and was taken into account in the analysis of the results. Due to the fact that for the design of the NVD
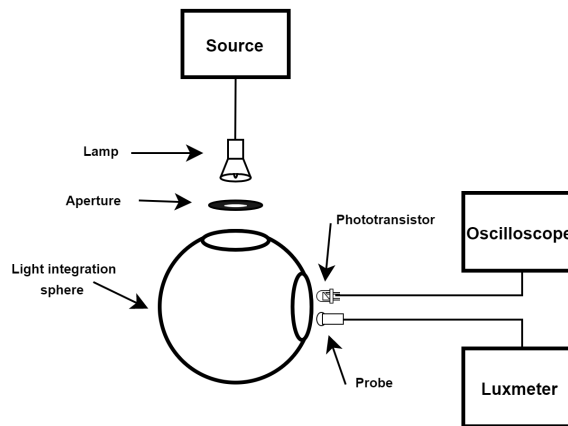
Fig. 4 Calibration workplace

photocathode protection, the illumination intensity versus time is the most important parameter and not the absolute values, this omission is not relevant to the results of this work [14].

2.3 Measurement of Flash Intensity

The experiment was conducted on a BREN 2 rifle with a 11-inch barrel, in caliber 5.56×45 mm. The muzzle device (flash suppressor) was removed. The layout of experiment is depicted in Fig. 2.

Only one type of cartridge and powder charge will be investigated in this work, as the goal of this work is to verify the possibility of using a designed measuring system. The ammunition of standard NATO type SS109 was used. The parameters of the ammunition used are shown in Tab. 1.

Twenty shot were fired with the described weapon and its ammunition. The result from all shots were reasonably similar and comparable, with a standard deviation of peak value to be $\sigma = 8.3 \times 10^4$ lux. One of the captured results are shown in Fig. 6.

By applying the calibration function to the measured voltage, we obtain the course of illumination as a function of time. The results are shown on the right side in Fig. 7. It can be seen from the recording that the maximum intensity of lighting reaches up to 2×10^5 lux. This value must be considered with a certain margin of error, because the sensitivity curve of the phototransistor used is strongly logarithmic, so even a small error in the measured voltage can cause a significant deviation of the resulting value.

Tab. 1 Cartridge parameters

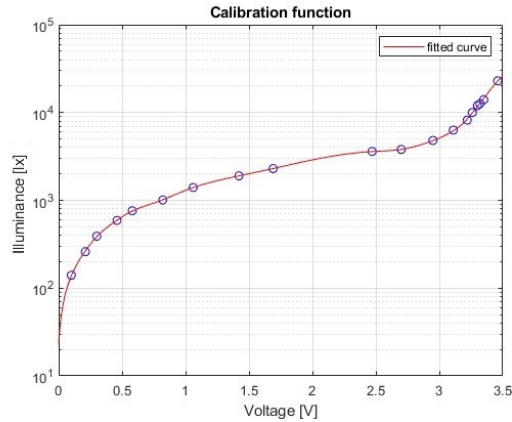| Cartridge type	Bullet type	Bullet weight	Primer	Powder type	Powder weight
5.56×45	SS109	4 g	4.4 Boxer	D073-03	1.5 g

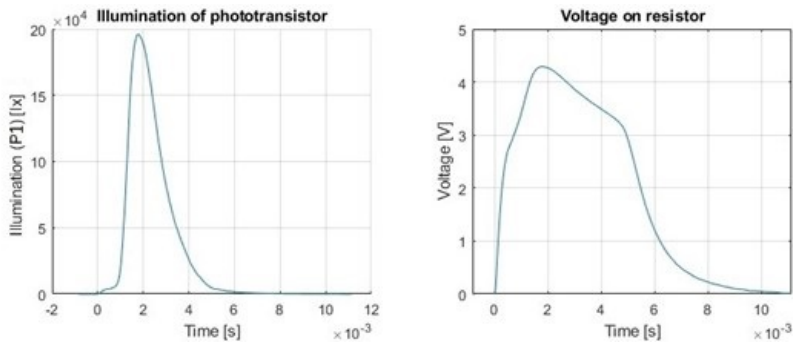*Fig. 5 Calibration curve of measuring chain*

Fig. 6 Example of measured results of muzzle flash intensity

2.4 Measurement of Autogating Delay

To analyze the function of the night device and to determine the autogating delay, a second measurement channel was implemented in the measurement chain. The phototransistor of this measuring chain was placed in the exit pupil of the night device. The MUM-14 device was used for the experiments. Although it is not a night vision sight, its construction is the same for purposes of this experiment. Moreover, this device was available to us and its possible damage (which is likely under the conditions of this experiment) was not undesirable. To eliminate a possible risk of damage or interference caused by physical recoil of weapon the MUM-14 device was mounted independently of the weapon, which is phenomenon that had been observed during a similar experiment in the past.

The measurement results are shown in Fig. 7. In the right part of the figure, there is a record of the measured voltage on the resistor. In the left part of the figure, this voltage is converted using the calibration function to the illumination level in lux. Data recorded in front of the NVD is shown in blue (PT1), while the data recorded behind the NVD is shown in red (PT2). In the left graph, two scales of illumination values were used, where
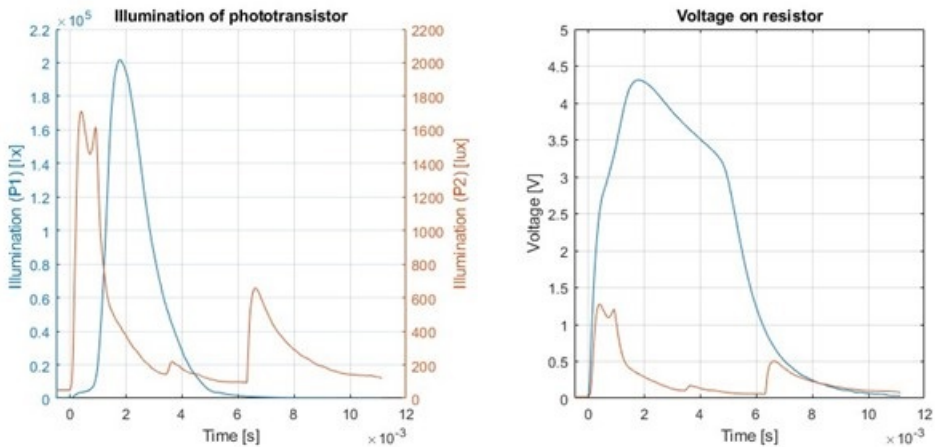
Fig. 7 Measured results of both phototransistors

the scale showing the illumination in the exit pupil of NVD is 10x smaller. This scale compression is forced by the nature of logarithmic calibration function.

The recording clearly shows the time-varying "amplification" of the illumination as it passes through the microchannel image brightness amplifier. In the detailed recording of the first two milliseconds, we can observe the response delay of the automatic brightness correction system and the autogating system. When the initial response of the control system occurs within 0.4 ms from the moment of the shot, the second reaction occurs at about 0.87 ms from the moment of the shot being fired. Details of the ABC system and autogating function are described in the literature. For the needs of the conceptual design of protection based on the basis of premature activation of autogating, information on the speed and time of the event is necessary. In this case, we consider 0.1 ms as the response limit. For a more accurate analysis and modeling, it would be necessary to carry out further experiments, which will be the subject of further research [1].

The autogating delay in the order of tens of microseconds observed in previous publication is probably the result of a different time constant of the phototransistor used [2]. Similar phenomena were observed in the experiment carried out as part of this publication, which had to be quantified and eliminated in subsequent data processing. According to the documentation, the type of phototransistor used has a time constant of 15 μs. When conducting the experiment, a great inconsistency in time constant was observed (twice as big as proclaimed by the manufacturer) for some pieces [2].

3   Possible Protection of IIT

Historically, the protection of the NVD during a shot was solved for larger weapons by an automatic aperture cover, which mechanically covered the lens for the necessary time when a shot was fired from a cannon or a rocket being launched. We can implement such protection only for large weapons, but not for automatic weapons. Such protection device may theoretically be possible to build and implement, but it would be too clumsy and unreliable for military application. Therefore another approach is suggests that just
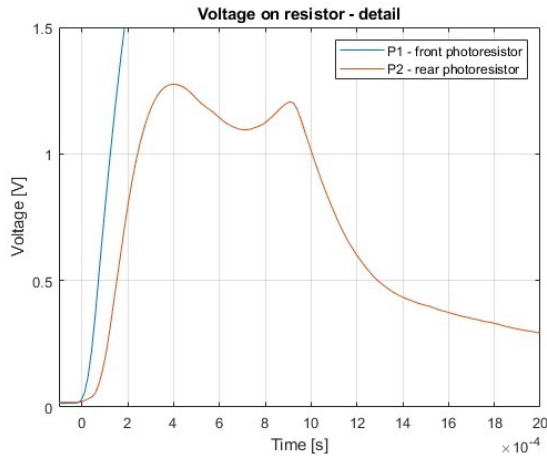
Fig. 8 Detail of ABC function during muzzle flash

before the shot, LED lights up in the field of view in close proximity in front of the lens, and it evenly illuminates the photocathode. The integrated protections of the MCP will be activated preemptively. The intensity of the LED lighting can be adequately regulated and set so that the LED itself does not cause damage to the MCP.

To activate the LED for preemptive activation of the integrated IIT protections, the use of a mechanical switch linked to the movement of the trigger, the firing mechanism or the bolt of the weapon seems to be the most appropriate place to attach sensor or switch. Considering the duration of the "lead time" for a long firearm (in the order of 0.008 - 0.01 s), this mechanical activation seems appropriate. The structural arrangement of this device in Fig. 9 will be the subject of further analysis in future publications.
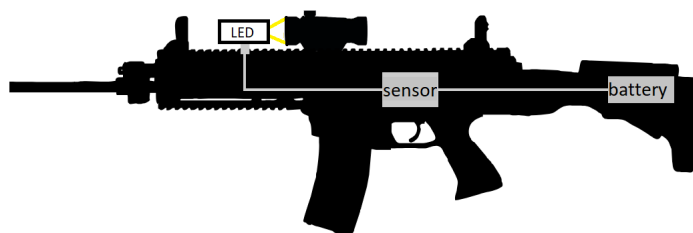

Fig. 9 Diagram of proposed NVD protection system

3.1 Model Example for MEO 50

The night sight MEO 50 was chosen as a model example because the design parameters of this lens are available to the authors. Thus, it is possible to model and calculate the

Tab. 2 MEO50 basic parameters

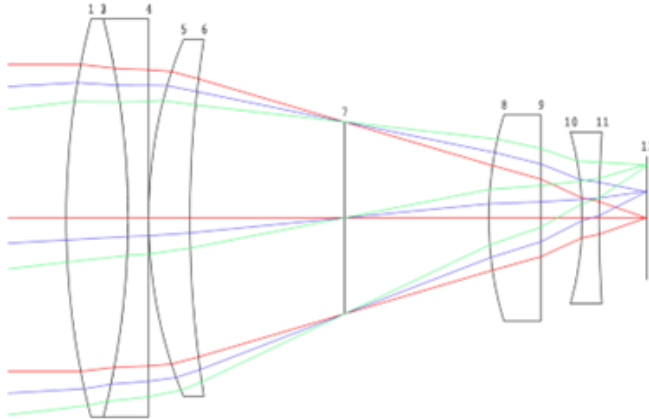| Focal length (mm)	Aperture number (-)	IIT diameter (mm)	Field of view angle
90	1.67	18	$2 \times 5.7°$

Fig. 10 Schematic diagram of lenses of MEO-50, with parallel rays [2]

exposure of the photocathode, the course and distribution of illumination on the photo-cathode. Modeling and calculations were carried out in the Optalix Software for Optical Design program. The basic technical data provided by the manufacturer are listed in the table below.

The IIT type XD - 4 is used in the sight, which is the same as in the MUM-14 device [15]. The NVD lens itself contains five optical lenses which are mineral lenses made of crown glass and flint glass. Parameter determinations and poly-chromatic modulation transfer function (MTF) values were calculated in Optalix Software for Optical Design. From the large range of spectral sensitivity of the receptor declared by the manufacturer, three wavelengths 546 nm, 650 nm and 850 nm, were deliberately chosen. Since the manufacturer states a field of view angle of $2 \times 5.7°$, the angles of incident light rays $0°$, $2.5°$ and $5°$ were chosen. Detailed parameters of each optical element are described in literature [2].

The resulting optical system of the MEO 50 lens is modeled in Fig. 10. The uniformity of photocathode irradiation was tested in the Optalix Software for Optical Design program using spot diagram. It was proven that the LED uniformly irradiates the entire IIT photocathode. Figure 11 shows the LED as a point source of radiation located in the object plane of the lens. The aperture angle of the beam is $10°$.

The second variant of possible active protection of the photocathode and MCP is the placement of the LED diode directly in the optical system of the lens between the optical
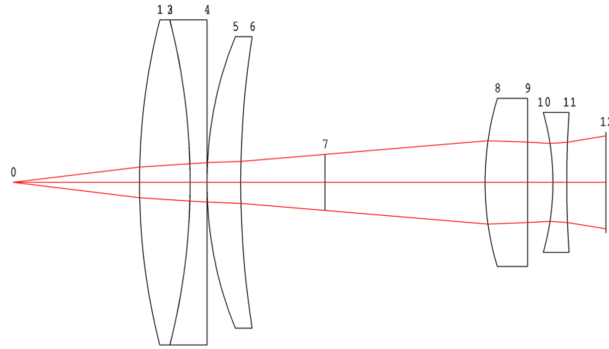
Fig. 11 Passage of protective LED rays – LED situated in point 0 [2]

elements. This would require an intervention in the design of the device, which is generally not desirable. This possibility is described in the literature [2].

3.2 Calculations for Verification of Established Photocathode Protection Designs

When choosing a suitable LED, for photocathode protection and MCP, it is important to note that the entire luminous flux falling on it will not pass through the input optical system. Energy losses occur in the optical system due to reflectance ρ, absorbance α, scattering σ and transmittance τ. The mentioned coefficients depend on the spectral composition of the incident radiation and on the properties of the materials of the optical elements. Energy losses in the optical system are expressed using the coefficient of internal transmission.

$$\tau_p = \prod_{j=1}^{k-1}(1-\rho_j) \tag{1}$$

where the transmittance coefficient takes into account only reflection losses;

$$\tau_\alpha = \prod_{j=1}^{k-1}(1-\alpha_j)^{d_j} = \prod_{j=1}^{k-1}(\tau_j)^{d_j} \tag{2}$$

And where the transmittance coefficient accounts for internal absorption. Energy losses on the input optical system can be suppressed by applying special layers to the optical elements.

If an anti-reflection layer is applied to the optical element, then approximately $\rho \approx$ 2% applies for one anti-reflective layer, $\rho \approx 1\%$ for three anti-reflection layers and $\rho \approx$ 0.5% for three anti-reflection layers.

Tab. 3 LED parameters

dominant wavelength [mm]	radiation angle [°]	power dissipation [mW]
625	50	105

Tab. 4 Optical properties of MEO-50 lens

Type of optical material	Refractive index of optical glass for λ = 632.8 nm	Internal transmittance tau depending on the thickness of the optical glass and the wavelength λ = 620 nm		d
		[10 mm]	[20 mm]	mm
N – BAK2	1.53806		0.994	12
N – SF57	1.83956	0.988		4
N – BAF8	1.60282	0.996		8
N – BAK4	1.56670		0.995	10.1
N – SF5	1.66848	0.995		33

The LED L – 934IT High Efficiency Red (GaAsP/ GaP) from Kingbright was chosen for the design of the photocathode protection option.

The closest wavelength with a known value of the refractive index and internal transmittance was used for the calculation. The optical system contains 8 surfaces at the interface with air and one cemented doublet. The parameters for calculating the transmittance coefficient are listed in Tab. 4.

Computation of transmittance coefficient taking into account only reflection losses are shown below.

$$\rho_1 = \frac{(n_1-1)^2}{(n_1+1)^2} = \frac{(1.53806-1)^2}{(1.53806+1)^2} = 0.0449 \tag{3}$$

$$\rho_2 = \frac{(n_2-1)^2}{(n_2+1)^2} = \frac{(1.83956-1)^2}{(1.83956+1)^2} = 0.0874 \tag{4}$$

$$\rho_3 = \frac{(n_3-1)^2}{(n_3+1)^2} = \frac{(1.60282-1)^2}{(1.60282+1)^2} = 0.0536 \tag{5}$$

$$\rho_4 = \frac{(n_4-1)^2}{(n_4+1)^2} = \frac{(1.56670-1)^2}{(1.56670+1)^2} = 0.0487 \tag{6}$$

$$\rho_5 = \frac{(n_5-1)^2}{(n_5+1)^2} = \frac{(1.66848-1)^2}{(1.66848+1)^2} = 0.0628 \tag{7}$$

$$\tau_\alpha = (1-\rho_1)(1-\rho_2)(1-\rho_3)(1-\rho_4)(1-\rho_5) = 0.6206 \tag{8}$$

Transmittance coefficient taking into account internal absorbance losses can be obtained.

$$\tau_\alpha = \prod_{i=1}^{5}(\tau_i^{d_i}) = 0.6206 \tag{9}$$

Transmittance coefficient τ of the lens without anti-reflective layers can then be calculated.

$$\tau = \tau_\rho \tau_\alpha = 0.5981 \tag{10}$$

The energy loss in an optical system without anti-reflective layers is approximately 40%. Meopta Group uses 2 to 3 anti-reflective layers. It follows that the total transmittance coefficient of the optical system is $\tau = 0.9594$. So the energy loss is only 4%. This is rapidly diminishing compared to a lens without anti-reflective coatings. The irradiation of the surface of the photocathode with a diameter of $D = 18$ mm, which is located in one plane with the LED, is calculated according to the following relationship:

$$E' = \frac{d\phi}{dA'}. \tag{11}$$

Where E' is the irradiance, dA' is the elemental area and $d\phi$ is the radiant flux. This basic relationship for the calculation of exposure will be modified for the purpose of the calculation.

Considering that the specific value, or ABC threshold on the luminescent screen is a few lux and the amplification coefficient, or MCP gain is $40\,000$, this selected LED is sufficient to trigger the protection systems in the IIT before the shot.

4   Conclusion

The experience suggests that NVD photocathode damage is more likely at maximum MCP gain. Based on the experimental measurements and the analysis of the captured data, it can be stated that the intensity of illumination falling on the lens of the device reaches up to 2×10^5 lux when fired from an assault rifle without a flame suppressor. This reading is extremely sensitive to the distance of the detection phototransistor from the muzzle of the weapon and the calibration of the measuring chain. The method described in this publication is not ideal for measuring the absolute value of illumination intensity. However, it can be used with great advantage to record the course of lighting intensity, or to analyze transient ballistics events. Figure 12 shows a photo taken during the experiment, clearly the demonstrating purpose of this paper.

The conceptual design of IIT protection using its integrated protections proved to be feasible. Depending on the considered lens and its optical properties, the protective LED parameters will of course differ. Limiting the field of view by inserting the described protective component (LED) is negligible. The connection of the protective LED and the mechanical function of the weapon will be the subject of further work. An alternative form of protection in the future may be the introduction of new types of powder charge and weapon design so that the powder particles are completely burned during the travel of the projectile in the barrel. Given the acquisition cost and current tactical requirements, it is unlikely that a complete rearmament to "low-flash" weapons will occur.

Fig. 12 Photo of experiment

Acknowledgement

References

[1] GRUZEVICH, Y.K. *Night vision opto-electronic devices (in Russian)*. Moscov: Fizmatlit, 2014. ISBN 978-9221-1550-6.

[2] BULINOVA, I. *Possibilities of protecting the photocathode of night sights of hand-held automatic weapons [diploma thesis](in Czech)*. Brno: Univerzita obrany, 2022.

[3] JUNEDUL, M. and M. MUNTJIR. Night Vision Technology: An Overview. *International Journal of Computer Applications*, 2017-06, **167**, pp. 37-42. DOI 10.5120/ijca2017914562.

[4] FISCHER, P., J. BUCHOLCER, T. BALAŽ, Z. ŘEHOŘ and F. RACEK. *Scriptum: Optical instruments II (in Czech)*. Brno: Univerzita obrany, 2004.

[5] *Photonics*. [online]. [viewed 2023-02-01]. Available from: www.photonis.com/products/image-intensifier-tube

[6] MCNAB, C., R. BUJEIRO and A. GILLILAND. *German automatic rifles 1941-45 : Gew 41, Gew 43, FG 42 and StG 44*. Osprey, 2013.

[7] PROCHÁZKA, S., P. SEMAN and M. VONDRÁČEK. Additional Effect of Gases on Strain Gauges at Barrel Muzzle. *Advances in Military Technology*, 2022-02, **6**(2), pp. 29-38. Available from: https://aimt.cz/index.php/aimt/article/view/1602

[8] KASTEK, M., R. DULSKI, P. TRZASKAWKA, T. PIA?TKOWSKI and H. POLAKOWSKI. Spectral measurements of muzzle flash with multispectral and hyperspectral sensor. *Proceedings of SPIE - The International Society for Optical Engineering*, 2011-06, **81933**. DOI 10.1117/12.900971.

[9] CARLUCCI, D.E. and S.S. JACOBSON. *BALLISTICS - THEORY AND DESIGN OF GUNS AND AMMUNITION*. USA: CRC Press, 2008. ISBN 978-1-4200-6618-0.

[10] SCHMIDT, E. M. and W.G. THOMPSON. *The effect of muzzle device configuration on the blast overpressure levels on the AH-1S Helicopter Tow Sight Unit*. Aberdeen Proving Ground, 1983.

[11] STEWARD, B.J., G.P. PERRAM and K.C. GROSS. Modeling midwave infrared muzzle flash spectra from unsuppressed and flash-suppressed large caliber munitions. *Infrared Physics & Technology*, 2012, **55**(4), pp. 246-255. ISSN 1350-4495. DOI https://doi.org/10.1016/j.infrared.2012.04.005.

[12] *LuckyLight - datasheet*. [online]. [viewed 2023-05-03]. Available from: www.tme.eu/cz/details/ll-503ptc2e-1ad/fototranzistory/luckylight/ [online]. [viewed 2023-05-03].

[13] VEKRBAUER, J. *Diploma thesis: Measurement of photometric characteristics of muzzle flash using a high-speed camera (in Czech)*. Brno: Univerzita obrany, 2022.

[14] CHRZANOWSKI, K. Review of night vision technology. *Opto-Electronics Review*, 2013-03, **21**. DOI 10.2478/s11772-013-0089-3.

[15] *Infrared MEO-50*. [online]. [viewed 2022-08-09]. Available from: www.infrared.cz/Produkty/Zamerovace/Meo50/